crystals

MDPI

Supplementary materials

Crystal Structure of IlvC, a Ketol-Acid Reductoisomerase, from *Streptococcus Pneumoniae*

Gyuhee Kim [1], Donghyuk Shin [1,3], Sumin Lee [2], Jaesook Yun [2] and Sangho Lee [1,*]

[1] Departments of Biological Sciences, Sungkyunkwan University, 2066 Seobu-ro, Suwon 16419, Republic of Korea; khyhies77@skku.edu (G.K.); shin@med.uni-frankfurt.de (D.S.); sangholee@skku.edu (S.L.)
[2] Departments of Chemistry, Sungkyunkwan University, 2066 Seobu-ro, Suwon 16419, Republic of Korea; go891209@nate.com (S.L.); jaesook@skku.edu (J.Y.)
[3] Max Planck Institute of Biophysics, Frankfurt am Main, 60438, Germany
* Correspondence: sangholee@skku.edu

Supplementary Table S1. Known KARI structures.

Class	Species	PDB ID	Resolution (Å)	Cofactors	Oligomeric State	Reference
			Gram-positive bacteria			
I	*Streptococcus pneumoniae*		1.69	NADPH, Mg^{2+}	Dimer	This study
I	*Slackia exigua*	4KQW	1.39	NADPH	Dimer	[1]
		4KQX [a]	1.80	NADPH, Mg^{2+}, IpOHA [b]	Dimer	[1]
I	*Alicyclobacillus acidocaldarius*	4TSK	2.60	NADPH, Mg^{2+}	Tetramer	[2]
I	*Mycobacterium tuberculosis*	4YPO	1.00	Mg^{2+}	Dimer	[3]
			Gram-negative bacteria			
I	*Pseudomonas aeruginosa*	1NP3	2.00		Dodecamer	[4]
II	*Escherichia coli*	1YRL	2.60		Tetramer	[5]
		3ULK	2.30	NADPH, Mg^{2+}	Tetramer	[6]
			Plants			
II	*Spinacia oleracea*	1YVE	1.65	IpOHA, NADPH, Mg^{2+}	Monomer	[7]
		1QMG	1.60	DMV [c], Mn^{2+}, ADP-ribose		[8]
II	*Oryza sativa Japonica Group*	3FR8	2.80	NADPH, Mg^{2+}	Monomer	[9]
		3FR7	1.55	Mg^{2+}	Monomer	[9]

[a] Engineerd mutant: S61D, S63D, I95V. [b] IpOHA, N-hydroxy-N-isopropyloxamate, a natural competitive inhibitor. [c] DMV, Dihyroxymethylvalerate (reaction product)

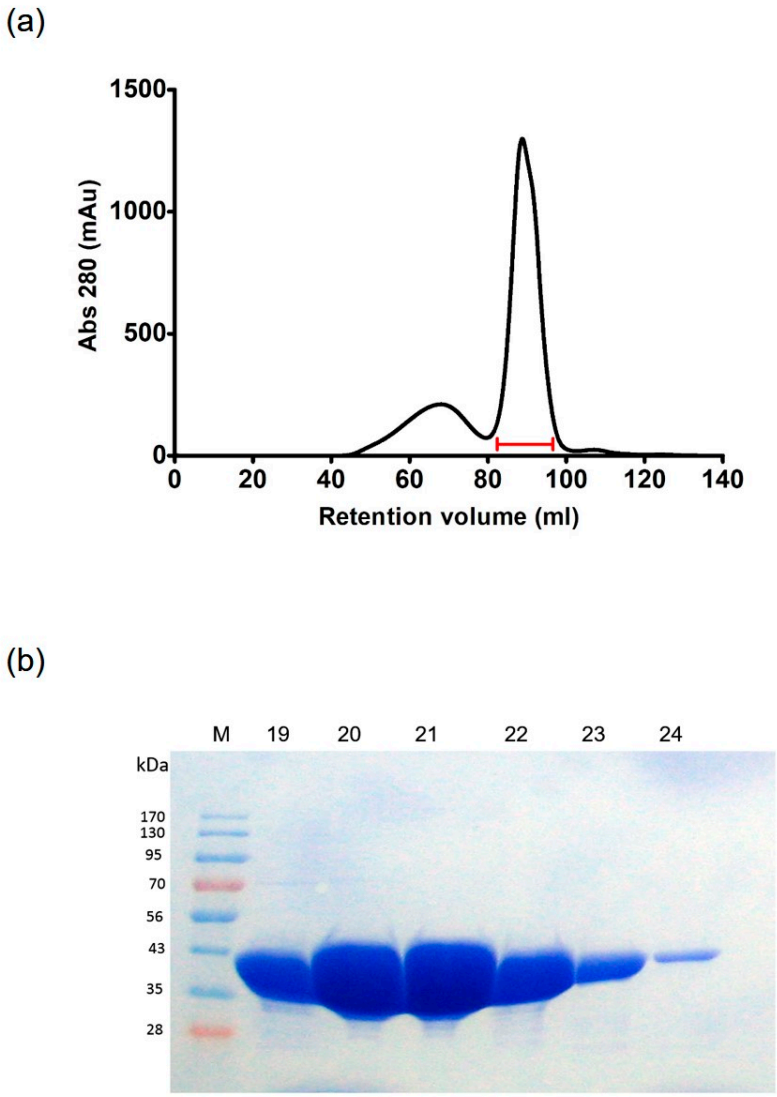

Supplementary Figure S1. Protein quality of SpIlvC. (a) A representative chromatogram of SpIlvC from a Superdex 200 size exclusion column (GE HealthCare). (b) SDS-PAGE analysis of fractions from a Superdex 200 column. Numbers indicate fraction numbers as shown in the panel (a).

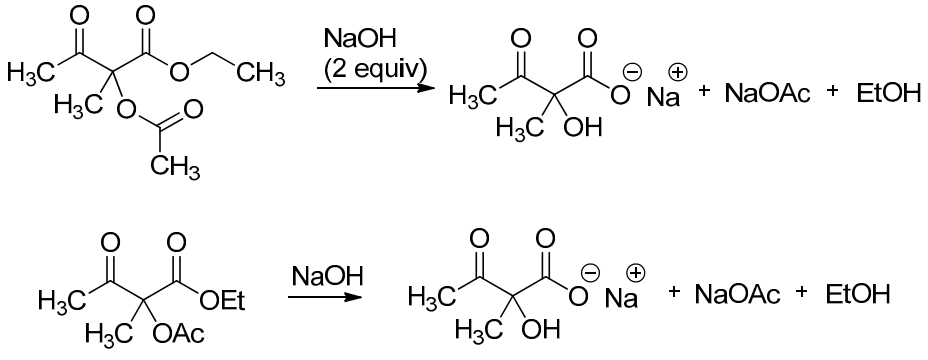

Supplementary Figure S2. Synthesis scheme of 2-acetolactate.

Reaction schemes for the synthesis of 2-acetolactate used as a substrate for the activity assay are shown.

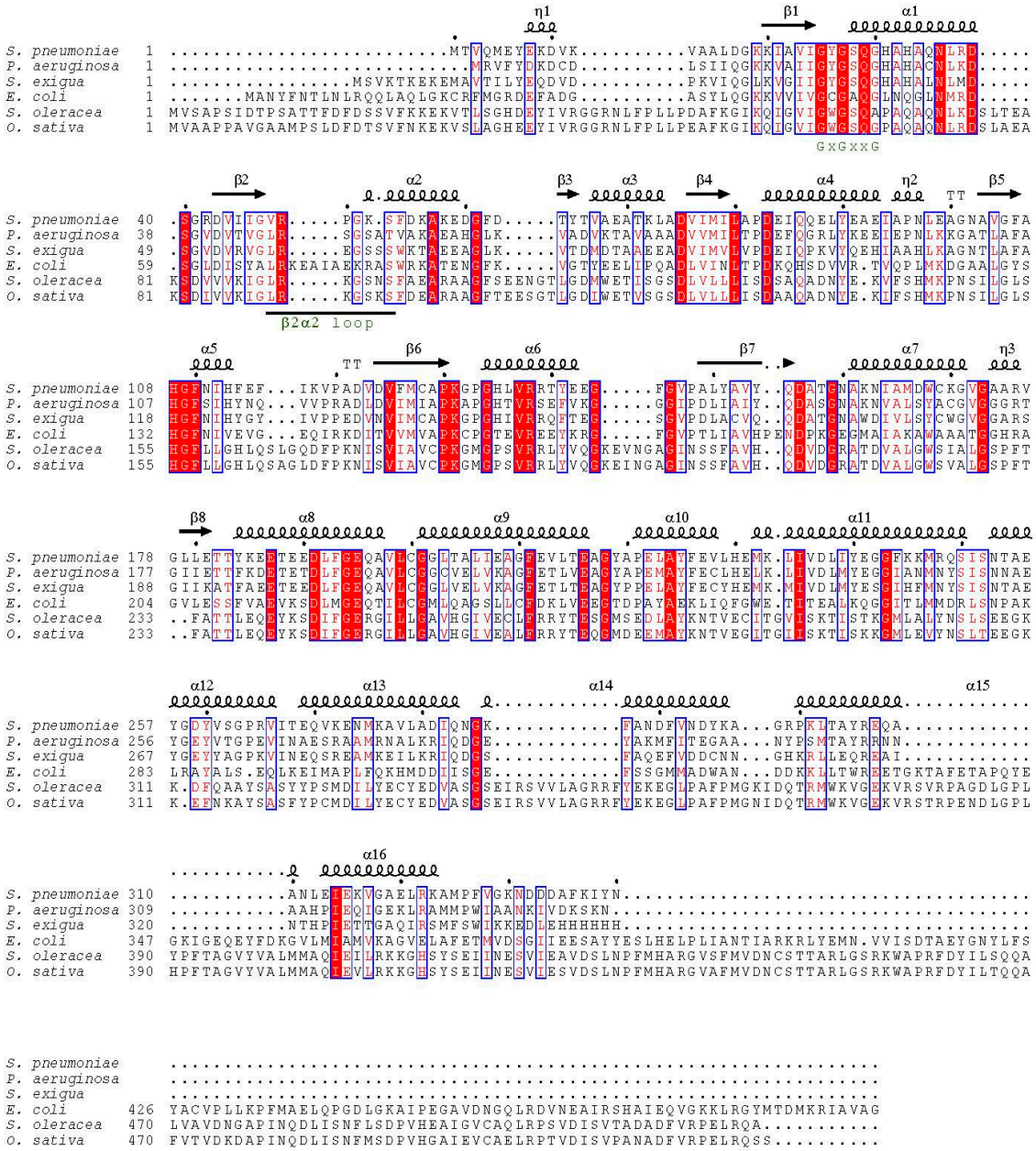

Supplementary Figure S3. Structure-based multiple sequence alignment of SpIlvC with KARIs from other organisms.

Multiple sequence alignment was prepared using *Clustal X2* [10] and *ESPript 3* [11]. The secondary structural elements of SpIlvC (α, α-helix; β, β-sheet; η, 3_{10} helix; and T, turn) were calculated using *ESPript 3*. Resides in blue-lined boxes indicate

consensus residues and red colored residues conserved ones.

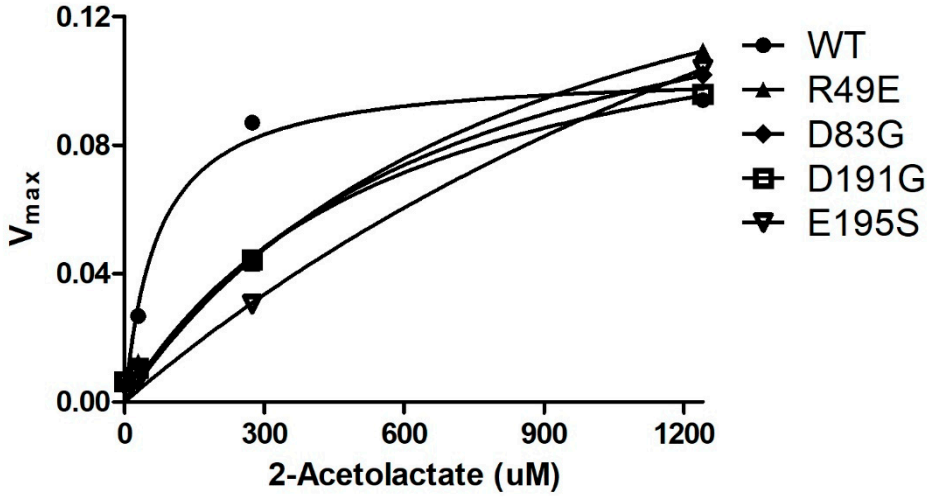

Supplementary Figure S4. Representative kinetics data of SpIlvC.

Reductase activity kinetics data are shown for those of SpIlvCwild-type (WT), NADP(H) binding site mutants (R49E and D83G) and Mg^{2+}-cooredingation site mutants (D191G and E195S).

Supplymentary References

1. Brinkmann-Chen, S., Flock, T., Cahn, J. K., Snow, C. D., Brustad, E. M., McIntosh, J. A., Meinhold, P., Zhang, L. & Arnold, F. H. (2013) General approach to reversing ketol-acid reductoisomerase cofactor dependence from NADPH to NADH, *Proc Natl Acad Sci U S A.* **110**, 10946-51.
2. Brinkmann-Chen, S., Cahn, J. K. B. & Arnold, F. H. (2014) Uncovering rare NADH-preferring ketol-acid reductoisomerases, *Metab Eng.* **26**, 17-22.
3. Lv, Y., Kandale, A., Wun, S. J., McGeary, R. P., Williams, S. J., Kobe, B., Sieber, V., Schembri, M. A., Schenk, G. & Guddat, L. W. (2016) Crystal structure of Mycobacterium tuberculosis ketol-acid reductoisomerase at 1.0 A resolution - a potential target for anti-tuberculosis drug discovery, *FEBS J.* **283**, 1184-96.
4. Ahn, H. J., Eom, S. J., Yoon, H. J., Lee, B. I., Cho, H. & Suh, S. W. (2003) Crystal structure of class I acetohydroxy acid isomeroreductase from Pseudomonas aeruginosa, *J Mol Biol.* **328**, 505-15.
5. Tyagi, R., Duquerroy, S., Navaza, J., Guddat, L. W. & Duggleby, R. G. (2005) The crystal structure of a bacterial class II ketol-acid reductoisomerase: domain conservation and evolution, *Protein Sci.* **14**, 3089-100.
6. Wong, S. H., Lonhienne, T. G., Winzor, D. J., Schenk, G. & Guddat, L. W. (2012) Bacterial and plant ketol-acid reductoisomerases have different mechanisms of induced fit during the catalytic cycle, *J Mol Biol.* **424**, 168-179.
7. Biou, V., Dumas, R., Cohen-Addad, C., Douce, R., Job, D. & Pebay-Peyroula, E. (1997) The crystal structure of plant acetohydroxy acid isomeroreductase complexed with NADPH, two magnesium ions and a herbicidal transition state analog determined at 1.65 A resolution, *EMBO J.* **16**, 3405-15.
8. Thomazeau, K., Dumas, R., Halgand, F., Forest, E., Douce, R. & Biou, V. (2000) Structure of spinach acetohydroxyacid isomeroreductase complexed with its reaction product dihydroxymethylvalerate, manganese and (phospho)-ADP-ribose, *Acta Crystallogr D Biol Crystallogr.* **56**, 389-97.
9. Leung, E. W. & Guddat, L. W. (2009) Conformational changes in a plant ketol-acid reductoisomerase upon Mg(2+) and NADPH binding as revealed by two crystal structures, *J Mol Biol.* **389**, 167-82.
10. Larkin, M. A., Blackshields, G., Brown, N. P., Chenna, R., McGettigan, P. A., McWilliam, H., Valentin, F., Wallace, I. M., Wilm, A., Lopez, R., Thompson, J. D., Gibson, T. J. & Higgins, D. G. (2007) Clustal W and Clustal X version 2.0, *Bioinformatics.* **23**, 2947-8.
11. Gouet, P., Courcelle, E., Stuart, D. I. & Metoz, F. (1999) ESPript: analysis of multiple sequence alignments in PostScript, *Bioinformatics.* **15**, 305-8.